Thermodynamic Basis for Engineering High-Affinity, High-Specificity Binding-Induced DNA Clamp Nanoswitches

Andrea Idili,[†,‡] Kevin W. Plaxco,[§,⊥] Alexis Vallée-Bélisle,[∥,*] and Francesco Ricci[†,‡,*]

[†]Dipartimento di Scienze e Tecnologie Chimiche, University of Rome, Tor Vergata, Via della Ricerca Scientifica, 00133, Rome, Italy, [‡]Consorzio Interuniversitario Biostrutture e Biosistemi "INBB", Rome, Italy, [§]Center for Bioengineering & Department of Chemistry and Biochemistry and [⊥]Interdepartmental Program in Biomolecular Science and Engineering, University of California, Santa Barbara California 93106, United States, and [∥]Laboratory of Biosensors and Nanomachines, Département de Chimie, Université de Montréal, Québec, Canada

ABSTRACT Naturally occurring chemoreceptors almost invariably employ structure-switching mechanisms, an observation that has inspired the use of biomolecular switches in a wide range of artificial technologies in the areas of diagnostics, imaging, and synthetic biology. In one mechanism for generating such behavior, clamp-based switching, binding occurs *via* the clamplike embrace of two recognition elements onto a single target molecule. In addition to coupling recognition with a large conformational change, this mechanism offers a second advantage: it improves both affinity and specificity simultaneously. To explore the physics of such switches we have dissected here the thermodynamics of a clamp-switch that recognizes a target DNA sequence through both Watson–Crick base pairing and triplex-forming Hoogsteen interactions. When compared to the equivalent linear DNA probe (which relies solely on Watson–Crick interactions), the extra Hoogsteen interactions in the DNA clamp-switch increase the probe's affinity for its target by ~0.29 ± 0.02 kcal/mol/base. The Hoogsteen interactions of the clamp-switch likewise provide an additional specificity check that increases the discrimination efficiency toward a single-base mismatch by 1.2 ± 0.2 kcal/mol. This, in turn, leads to a 10-fold improvement in the width of the "specificity window" of this probe relative to that of the equivalent linear probe. Given these attributes, clamp-switches should be of utility not only for sensing applications but also, in the specific field of DNA nanotechnology, for applications calling for a better control over the building of nanostructures and nanomachines.

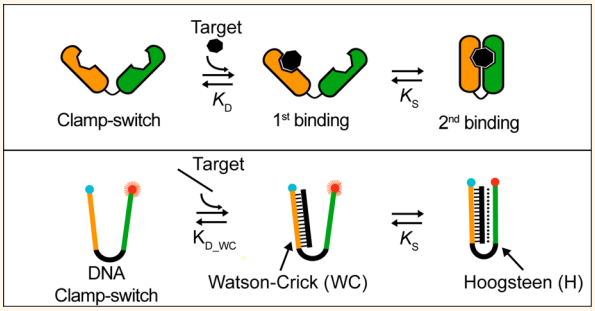

KEYWORDS: clamp mechanism · triplex · DNA nanomachines · biomolecular switch · molecular beacons · specificity · ligand-induced fit

The use of binding-induced conformational changes to transduce binding events into useful outputs is ubiquitous throughout the cell. Protein- and RNA-based biomolecular switches, for example, undergo binding-induced changes in conformation or oligomerization and use this information to transduce chemical information into specific biochemical outputs. Motivated by the impressive performance of these naturally occurring biomolecular switches, significant effort has gone into the design of similar switches for use in artificial biotechnologies, including molecular diagnostics, synthetic biology, and imaging.[1−11]

Two general strategies are typically employed for engineering binding-induced molecular switches (Figure 1). The first strategy consists in re-engineering a recognition element so that it adopts a *distorted* conformation incapable of binding the target (the *nonbinding* "*off*" state; Figure 1, top). This is typically achieved by stabilizing an alternative, nonbinding state *via* the addition of non-native interactions. In the presence of a target ligand this *nonbinding* "*off*" state, which is in equilibrium with the *binding-competent* "*on*" state, shifts toward the latter state *via* a *population-shift* mechanism.[2,12−16] The observed affinity of such a switch is thus decreased as the

* Address correspondence to francesco.ricci@uniroma2.it, a.vallee-belisle@umontreal.ca.

Received for review August 17, 2013 and accepted November 12, 2013.

Published online November 12, 2013
10.1021/nn404305e

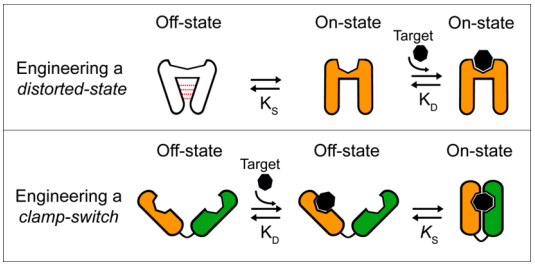

Figure 1. Two general strategies used to design binding-induced molecular switches. (Top) Recognition element can be re-engineered into a switch by introducing *non-native* interactions (red dotted lines) that stabilize a distorted, *nonbinding "off"* state. Upon target binding, the equilibrium between this distorted state and the *binding-competent "on"* state, K_S, is switched to the latter state *via* a *population-shift* mechanism.[22] The observed affinity (K_{D_obs}) of such switch is thus arbitrarily decreased as K_S is reduced (i.e., as the stability of the *non-native* interactions increases) *via* the following relationship: $K_{D\_obs} = K_D((1+K_S)/K_S)$, where K_D is the affinity of the binding-competent state for the target. (Bottom) Alternatively, *clamplike* switches can be built by fusing together two recognition elements that embrace a single copy of the target in a complementary manner.[5,8] In this mechanism, the affinity of the switch for its target increases proportionally with K_S (i.e., with the stability of the additional interactions) *via* the following relationship: $K_{D\_obs} = K_D/(1 + K_S)$. We recently described the thermodynamic basis for the design and optimization of biomolecular switches of the first type,[22] providing a rational path to control and tune the sensitivity of many DNA-based probes.[23−26] Here, we similarly explore the thermodynamic basis for building biomolecular switches of the second type.

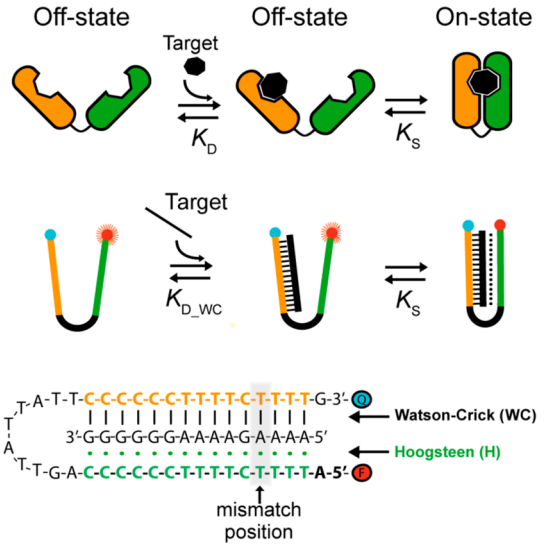

Figure 2. Use of a model DNA-based nanoswitch to understand the thermodynamic basis of the enhanced affinity and specificity of clamp-switches. This DNA switch is composed of two recognition domains separated by an unstructured 10-base loop. The first recognition domain (orange sequence) recognizes the target *via* Watson−Crick base pairing. Upon target binding, the double-stranded DNA is then recognized by the second recognition domain (a triplex forming oligonucleotide, TFO, shown in green) through Hoogsteen base pairs, leading to the formation of a triplex DNA structure. To generate a measurable output, the switch is modified with a fluorophore/quencher pair that is brought into proximity upon formation of the triplex structure (signal-off). The affinity and specificity of such clamp-switches have been compared with those of a simple, linear DNA sequence that recognizes its target solely *via* Watson−Crick base pairing (nonswitching probe, Figure S3, Supporting Information) and that share the same common recognition element (orange strand). The linear nonswitching probe was also labeled with a fluorophore and a quencher at the two ends to observe a measurable output upon target binding.

stability of the non-native interactions increases. The second strategy used for designing binding-induced molecular switches consists in engineering a *clamplike* mechanism that employs two recognition elements that embrace a single copy of the target (Figure 1, bottom),[5,8,17,18] thus leading to enhanced affinity (due to the larger recognition interface).[17−21] Moreover, because clamp-switches recognize a single region of their target using multiple recognition elements, this improvement in affinity generally comes with an improvement in the gap between the affinity of the proper target and that of mismatched targets, thus potentially enhancing specificity.

While biomolecular switches of the first type,[22] have been thoroughly characterized, providing a rational path toward their design and optimization,[22−26] the clamplike mechanism, despite its promising properties, has seen much less investigation efforts. Thus motivated, we explore here the thermodynamic basis for the design and optimization of clamplike biomolecular switches. We do so using a model DNA-based nanodevice that recognizes a target oligonucleotide *via* both Watson−Crick base pairing and triplex-forming Hoogsteen interactions (Figure 2).

RESULTS AND DISCUSSION

As our test bed we have employed a simple, DNA-based clamp-switch composed of two recognition elements separated by an unstructured, 10-base loop (for other, similar examples see refs 27−31 and references therein). The first recognition element, a 15-base polypyrimidine sequence (Figure 2, in orange), binds the target, a polypurine sequence, *via* Watson−Crick base pairing. The second recognition element, a polypyrimidine sequence (Figure 2, in green), then binds the so-formed duplex *via* sequence-specific Hoogsteen base pairing.[32,33] The formation of this triplex conformation occurs through a structure-switching mechanism that leads to the switch's closure.[27−31,34−36] In support of this proposed mechanism, we note that, in the absence of complementary base pairing between the two recognition elements, we observe the switch's closure only in the presence of the target (Figure S1, Supporting Information). The switch's affinity toward a specific target is also strongly decreased at high pH or in the absence of Mg^{2+}, conditions known to disrupt Hoogsteen interactions[27,28] (Figure S2, Supporting Information).

The affinity of the clamp-switch for its target (K_{D_clamp}) depends on Watson−Crick (K_{D_WC}) and Hoogsteen base pair interactions (this latter determining the switching

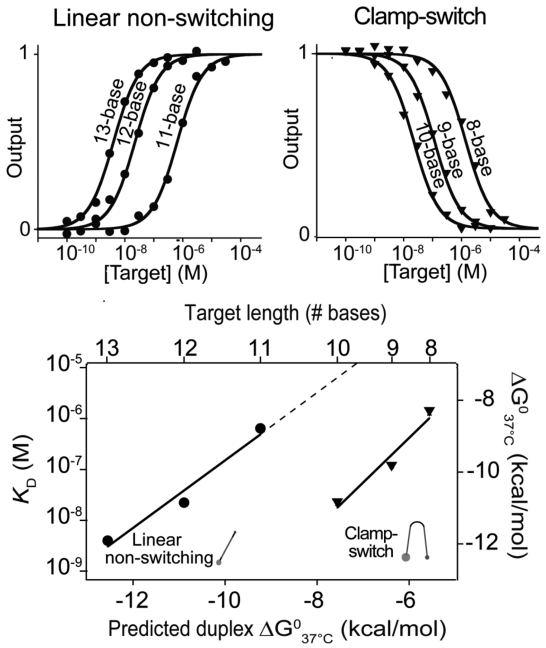

Figure 3. Affinity of the clamp-switch (top, right) is greater than that of the linear nonswitching probe (top, left), enough so that a target must be ~20% longer to bind the later as tightly. (Bottom) Shown are the experimentally derived affinities (and the equivalent free energies) of a clamp-switch and a linear nonswitching probe using the same Watson–Crick recognition element versus target length (and the nearest neighbor model predicted binding energy).[37–39] The binding curves were obtained by adding increasing concentration of perfectly matched targets of different length to a 2 nM concentration of clamp-switch (top, right) or linear nonswitching (top, left) probe in 100 mM Tris buffer, 10 mM $MgCl_2$, pH 7.0 at 37 °C.

equilibrium constant, K_S), *via* the following equation:

$$K_{D_{clamp}} = \frac{K_{D_{WC}}}{1 + K_S} \quad (1)$$

To dissect the thermodynamics of this clamp-switch, we have compared its affinity and specificity to those of a simple, linear DNA sequence that recognizes its target solely *via* Watson–Crick base pairing and that does not undergo any (energetically significant) conformational change (*nonswitching* probe, Figure S3, Supporting Information). For ease of comparison both probes share a common recognition element (orange strand in Figure 2). Because the linear probe does not undergo a structural switch and only forms Watson–Crick base pairing, it can be used to determine K_{D_WC} (see Figure 2). Together with the affinity of the clamp-switch probe (K_{D_clamp}), this value provides a route to evaluating the contribution of the switching mechanism (K_S) of the clamp-switch using eq 1.

Clamp-switch probes bind to their targets with greater affinity than do the equivalent linear DNA probes (Figure 3 and Figure S4, Supporting Information).[27–31,34–36] Indeed, the improvement in affinity is so great that we cannot directly measure the difference in binding energies for any single target. That is, because the affinity of the probes we tested can only be quantitatively measured over a specific concentration window, which is found between the concentration of the switch/probe (i.e., 2 nM) and the highest concentration of target that can be reasonably added to the working solution (here 0.1 mM), there is no single target for which both probes produce measurable dissociation constants. For example, while the clamp-switch exhibits micromolar affinity with a target as short as eight bases (K_{D_clamp} (8-base) = 1.4 μM; Figure 3, right), the linear nonswitching probe does not exhibit any detectable binding with this same target at even the highest concentrations we have tested (100 μM). We have thus instead used extrapolations from data we collected to estimate the difference in the free energy with which each probe would bind a specific, 10-base target. We have taken two approaches to this end. The first is based on the observation that the affinity of the clamp-switch for a 10-base target matches the affinity with which the linear nonswitching probe binds a longer, 12-base target (K_D = 20 nM; Figure 3). A nearest neighbor model[37–39] predicts that these two extra G–C Watson–Crick base pairs should provide an additional 3.3 kcal/mol in binding energy, suggesting that this represents the extra stabilization provided by the Hoogsteen base pairing between the clamp-switch and the 10-base target. As a second means of estimating the Hoogsteen base-pairing contribution we predict the free energy with which the linear probe binds a 10-base target by extrapolation of the experimental data obtained with the same probe for longer targets (Figure 3, bottom). The difference between this extrapolated value (7.7 kcal/mol) and the experimental value for the clamp-switch binding to this same 10-base target (10.9 kcal/mol) is, at 3.2 kcal/mol, in good agreement with the value achieved with the first approach.

Given that, at pH 7, the free energy of forming a CGC Hoogsteen base pairs is nearly equal to that of forming a TAT Hoogsteen interaction,[40,41] the 3.3 kcal/mol additional energy provided by the extra 10 Hoogsteen base pairs in the clamp-switch suggests that each Hoogsteen base pair provides ~0.33 kcal/mol/base in stabilization, which is in close agreement with previous reports.[40,42] The 3.3 kcal/mol in additional binding energy provided by the 10 extra Hoogsteen base-pairs also corresponds to a clamp-switch equilibrium constant, K_S, of 190. This, as expected (eq 1) improves the affinity of the clamp-switch by ~200-fold relative to that of the linear probe.

The enhanced affinity of the clamp-switches is not found in other mechanisms of coupling binding to a large-scale conformational change. Specifically, the affinity of clamp-switches is greater than that of the equivalent (i.e., same recognition site) switch, which uses the other commonly employed switching mechanism: an engineered distorted state (Figure 1, top).

To show this we have compared the clamp-switch with the equivalent molecular beacon, a commonly employed optical or electrochemical approach for the detection of specific DNA sequences.[1,43−45] A molecular beacon is a fluorophore-and-quencher-modified DNA strand that forms a low-emissive stem-loop conformation due to hybridization of its complementary ends. This structure opens, thus producing enhanced fluorescence, when a target hybridizes to the loop, breaking the stem and segregating the fluorophore/quencher pair (Figure S3, Supporting Information). In contrast to the nanomolar affinity that the clamp-switch shows for targets as short as 10 bases, the molecular beacon does not reach this affinity until targets of at least 15 bases are used (Figure S5, Supporting Information). This occurs because molecular beacons employ an engineered distorted state (here a stem-loop structure), the stabilization energy of which competes with target binding (Figure S3, Supporting Information). This effect is more readily apparent if we compare the affinity of the linear probe and the equivalent molecular beacon since we are able to compare directly the affinities of these probes for a single target of the same length (i.e., 13 bases). While the linear nonswitching probe shows nanomolar affinity (K_D = 4 nM) for a 13-base target, the affinity of the molecular beacon for this same target is some 40-fold poorer (K_D = 162 nM) (Figure 3 and Figure S5, Supporting Information).

In addition to improve binding affinity, the clamp-switch mechanism should, at least in principle, also enhance specificity.[17−21] To explore this we have compared the affinities of our clamp-switch against a perfectly matched and a single-base mismatched target (see Figure 2 for mismatch location). In order to describe specificity quantitatively we use the discrimination factor, *Q*, which is the ratio of the output signal produced by the perfectly matched target (χ_{PM}) to that of the mismatched target (χ_{MM}) (Figure 4)[46] and the specificity window, defined here as the range of target concentration at which we observe a value of *Q* equal or above 5 (thus representing a 20% interfering signal). The specificity window of the simple linear nonswitching probe spans about an order of magnitude in target concentration (Figure 4, bottom). The specificity window of the clamp-switch, in contrast, is 10 times wider (Figure 4, top). Due to the experimental limitations described above, however, the specificity of the clamp-switch probe was determined using a shorter target (10-base) than that employed to test the specificity of the linear nonswitching probe (13-base) which could, in theory, also lead to higher specificity. To rule this out, we performed simulations using the nearest neighbor model,[37−39] which confirm that the small difference in target length does not account for the large difference in specificity we observe (Figure S6, Supporting Information).

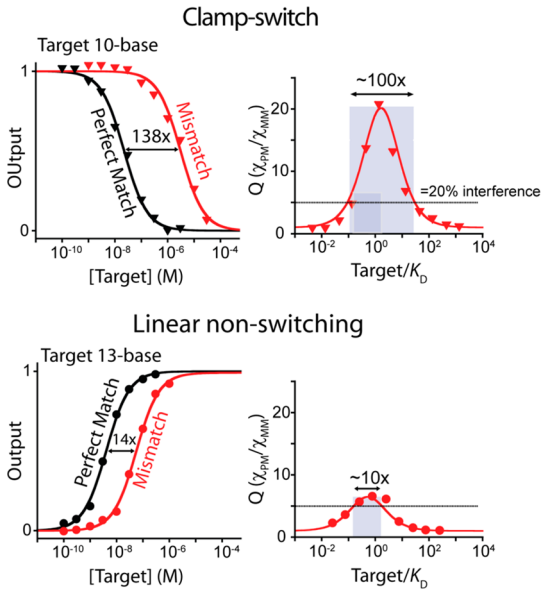

Figure 4. Additional Hoogsteen base pairs in our clamp-switch (top) increase the probe's specificity by 10-fold over that of the equivalent simple linear nonswitching probe (bottom). To demonstrate this we challenged both probes against a perfectly matched target and a single-base mismatched target. Shown (right-hand column) is the discrimination factor, *Q*, the ratio between perfect match and mismatch outputs, as a function of target concentration. We have also highlighted the specificity window (gray rectangles), defined here as the range of target concentration at which we observe a value of *Q* equal or above 5 (thus representing a 20% interfering signal). This window is more than 1 order of magnitude broader for the clamp-switch. These binding curves were obtained by adding increasing concentration of perfectly matched and 1-base mismatched DNA targets to a 2 nM concentration of clamp-switch (top) or linear nonswitching (bottom) probe in 100 mM Tris buffer, 10 mM $MgCl_2$, pH 7.0 at 37 °C.

The different specificity windows of the two probes provide an additional insight on how the clamp-switch mechanism leads to enhanced specificity. Specifically, the 138-fold difference in affinity between the perfectly matched and the single-based mismatched target for the clamp-switch suggests that the mismatch is 3.10 kcal/mol less stable than the perfectly matched target (Figure 4). For the linear probe, in contrast, the 14-fold difference in affinity between the perfectly matched and the mismatched target gives a mismatch destabilization of only 1.66 kcal/mol. The extra Hoogsteen interactions in the clamp mechanism thus improve the specificity of the clamp-switch by ca. 1.44 kcal/mol.

In contrast to the clamp-switch mechanism, the distorted recognition element strategy does not enhance specificity over that of the nonswitching linear probe. The stem-loop distorted switch (i.e., the molecular beacon; see Figure S3, Supporting Information), for example, exhibits a specificity window similar to the one of the linear nonswitching probe (Figure S7, Supporting Information). This is likely attributable to the fact that the non-native interactions introduced in

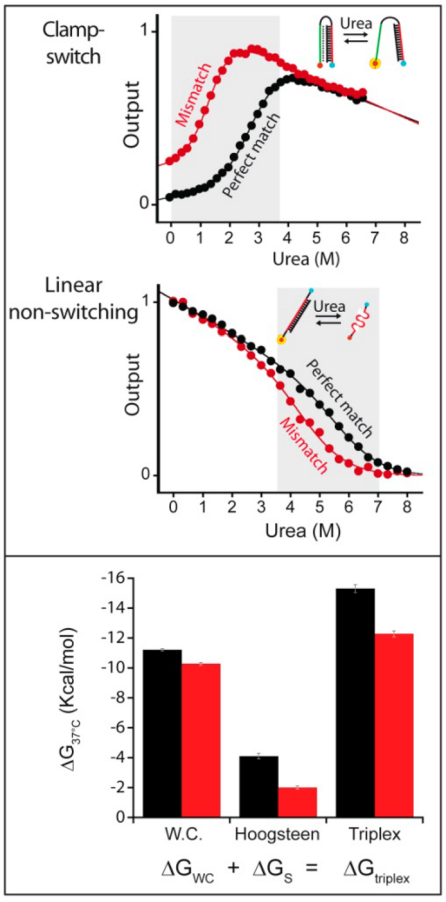

Figure 5. Urea denaturation curves (see the Supporting Information for more details) provide a means by which to compare both the specificity and affinity of the clamp-switch probe with those of the equivalent, nonswitching linear probe using a single 14-base perfect match/mismatch target pair (both at a saturating concentration of 10 μM). Note that the unfolding/dissociation of the clamp-switch occurs at much lower urea concentrations, thus suggesting a sequential unfolding of the triplex probe through (1) denaturation of the triplex Hoogsteen interactions followed by (2) denaturation of the remaining duplex. We determined ΔG_{WC}, the free energy of association of the linear probe for both the perfect match (11.2 $\pm$ 0.1 kcal/mol) and the mismatch (10.3 $\pm$ 0.1 kcal/mol) (see the Supporting Information, eq 7). Using a two-state approximation (see the Supporting Information, eq 13), we found that the clamp-switch free energy of opening (Hoogsteen interactions), ΔG_S, is 4.1 $\pm$ 0.2 kcal/mol and 2.0 $\pm$ 0.1 kcal/mol for the perfect match and mismatch target, respectively. We note that the 4.1 $\pm$ 0.2 kcal/mol is in excellent agreement with the results obtained using binding curve analysis (0.29 $\pm$ 0.02 kcal/mol/base ~4.1 kcal/mol/14-bases; Figure 3). The difference in free energies for perfect match and mismatch targets obtained with the linear probe (11.2 ($\pm$0.1) − 10.3 ($\pm$0.1) = 0.9 $\pm$ 0.1 kcal/mol) and the clamp-switch (4.1 ($\pm$0.2) − 2.0 ($\pm$0.1) = 2.1 $\pm$ 0.2 kcal/mol) are also in good agreement with the results obtained above from extrapolations of the binding curve (Figure 4) and confirm the enhanced specificity of the clamp-switch relative to the linear, nonswitching probe.

this class of switches do not alter the binding interface between the switch and the target (Figure 1, top).[25]

To further explore the improved performance of clamp-switches we have also employed urea denaturation experiments, which provide a route toward determining their switching and binding thermodynamics[22,47−49] (Figure 5, and see the Supporting Information for detailed information about this method). An advantage that such experiments have over the more traditional measurement of binding curves is that they provide a means of determining the free energy of association between two biomolecules in presence of saturating amount of one of them. The approach thus allows us to compare the free energy of association of the clamp-switch and linear probes when each is bound to the same target. Using this approach, we find that the difference in free energy with which the clamp-switch binds mismatched and perfectly matched targets is, at 2.1 $\pm$ 0.2 kcal/mol, significantly higher than the 0.9 $\pm$ 0.1 kcal/mol difference observed for the linear nonswitching probe (Figure 5). Of note, this extra 1.2 $\pm$ 0.2 kcal/mol in discrimination energy provided by the Hoogsteen interactions in the clamp-switch agrees well with the value determined above using binding curves (i.e., 1.44 kcal/mol). The 4.1 $\pm$ 0.2 kcal/mol (0.29 $\pm$ 0.02 kcal/mol/base) additional interaction energy provided by the 14 Hoogsteen interactions in the clamp-switch is likewise close to the ~0.33 kcal/mol/base value estimated from the extrapolation procedure using the 10-base target (Figure 3).

CONCLUSION

In this work, we have explored the thermodynamics by which *clamp-based* molecular switches improve both the affinity and specificity of recognition.[18−22,27−31,34−36] Using a simple DNA model clamp-switch, the triplex-forming probe, we showed that clamp-switches recognize their specific target through two sequential binding events which sum up to provide a higher binding free energy and greater discrimination efficiency than those observed for either the equivalent, nonswitching linear probe or a switch based on the engineering of a distorted state. These advantages likely explains why evolution employs clamplike strategies so frequently when it builds its signaling mechanisms.[8,50−52]

The simplicity of the clamp-switch strategy may also inspire us toward engineering switches with improved affinity and specificity. For example, binding-activated molecular probes could be engineered to detect DNA sequences with much higher specificity than those based on simple Watson−Crick base pairing. Of note, triplex forming sequences are common enough that it is straightforward to select unique sites in human or pathogen genomes.[52,53] In addition, the clamp-switch strategy dissected here could also be used to engineer highly specific structure-switching biosensors using more complex recognition elements that can include aptamers[54] and proteins.[17−21] Finally, with their ability to detect very short targets with high

affinity and specificity, DNA clamp-switches should find many applications for building new DNA nanostructures, DNA nanomachines and DNA origami,[55−61] where the ability to specifically and tightly bind short DNA sequences will lead to improved structural control.

MATERIALS AND METHODS

HPLC-purified oligonucleotides labeled with a FAM (5-carboxyfluorescein) at the 5′ end and a BHQ-1 (black hole quencher 1) at the 3′ end were purchased from Sigma-Genosys. We used a triplex-clamp switch, a linear probe and a molecular stem-loop beacon all of them bearing the same 15-base recognition element. The sequences of the probes were as follows.

Triplex clamp-switch: 5′-A-*TTTTCTTTTCCCCCC*-AGTTATTATT-**CCCCCCTTTTCTTTT**-G-3′

Linear nonswitching probe: 5′-A-**CCCCCCTTTTCTTTT**-G-3′

Molecular beacon: 5′-A-CTCGC-**CCCCCCTTTTCTTTT**-GCGAG-G-3′

For all the sequences above the bases in bold represent the recognition element (red portion in Figure S3, Supporting Information). In the molecular beacon sequence above the underlined bases represent the stem portion (black and green portion in Figure S3, top, Supporting Information). In the clamp-switch the underlined bases represent the random loop sequence (black portion in Figure 2) and the italic bases represent the triplex forming oligonucleotide sequence (green portion in Figure 2). The sequences, sensing principles and the expected conformational change of the three probes used in this work are depicted in Figure S3 (Supporting Information).

Perfect match and mismatch targets were also purchased from Sigma-Genosys. The sequences of the probes were as follows.

Perfect match targets:

15-base: 5′-AAAAGAAAAGGGGGG-3′
14-base: 5′- AAAAGAAAAGGGGG-3′
13-base: 5′- AAAAGAAAAGGGG-3′
12-base: 5′- AAAAGAAAAGGG-3′
11-base: 5′- AAAAGAAAAGG-3′
10-base: 5′- AAAAGAAAAG-3′
9-base: 5′- AAAAGAAAA-3′
8-base: 5′- AAAAGAAA-3′
7-base: 5′- AAAAGAA-3′

Mismatch targets have the same sequence of the perfect match targets except for a mutated base in position 4 where the A base was substituted with a C base. For example, for the 14-base mismatch target the sequence was as follows

14-base: 5′- AAACGAAAAGGGGG-3′

where the underlined base represents the mismatch position.

All experiments were conducted in 100 mM Tris buffer, 10 mM $MgCl_2$, pH 7.0 at 37 °C unless otherwise stated. All fluorescence measurements were obtained using a Cary Eclipse Fluorimeter with excitation at 480 (±5) nm and acquisition between 514 and 520 nm. Ultrapure urea was obtained from Sigma-Aldrich. Urea unfolding curves were obtained using 10 nM of the relevant probe (clamp-switch or linear probe) by sequentially increasing the urea concentration of a 0 M urea sample with 8 M urea containing the same concentration of probe. The fluorescence of the open state was set relative to 1.

Binding curves were obtained using 2 nM of the relevant probe (clamp-switch, linear or stem-loop probe) and were fitted to a single-site binding mechanism ([X] = target concentration; F_B = fluorescence in the presence of saturating concentration of target; $F_{[T]}$ = fluorescence in the presence of different concentration of target; F_0 = background fluorescence):

$$F_{[T]} = F_0 + \frac{[X](F_B - F_0)}{[X] + K_D} \quad (2)$$

Conflict of Interest: The authors declare no competing financial interest.

Supporting Information Available: Supplementary figures. This material is available free of charge *via* the Internet at http://pubs.acs.org.

Acknowledgment. This work was supported by the Bill & Melinda Gates Foundation through the Grand Challenges Explorations (OPP1061203) (F.R.), by the International Research Staff Exchange Scheme (IRSES) grant under the Marie Curie Actions program (F.R.), by the NIH through Grant No. R01EB007689 (K.W.P.), and by the National Sciences and Engineering Research Council of Canada through Grant No. 436381-2013 (AVB). F.R. is supported by a Marie Curie Outgoing Fellowship (IOF) (Proposal No. 298491 under FP7-PEOPLE-2011-IOF). A.I. is supported by the Canada−Italy innovation award.

REFERENCES AND NOTES

1. Tyagi, S.; Kramer, F. R. Molecular Beacons: Probes That Fluoresce Upon Hybridization. *Nat. Biotechnol.* **1996**, *14*, 303–308.
2. Vallée-Bélisle, A.; Plaxco, K. W. Structure-Switching Biosensors: Inspired by Nature. *Curr. Opin. Struct. Biol.* **2010**, *20*, 518–526.
3. Radley, T. L.; Markowska, A. I.; Bettinger, B. T.; Ha, J. H.; Loh, S. N. Allosteric Switching by Mutually Exclusive Folding of Protein Domains. *J. Mol. Biol.* **2003**, *332*, 529–536.
4. Stratton, M. M.; Mitrea, D. M.; Loh, S. N. A Ca^{2+}-Sensing Molecular Switch Based on Alternate Frame Protein Folding. *ACS Chem. Biol.* **2008**, *3*, 723–732.
5. Stratton, M. M.; Loh, S. N. Converting a Protein Into a Switch for Biosensing and Functional Regulation. *Protein Sc.* **2011**, *20*, 19–29.
6. Wright, C. M.; Heins, R. A.; Ostermeier, M. As Easy as Flipping a Switch? *Curr Opin. Struct. Biol.* **2007**, *11*, 342–346.
7. Ostermeier, M. Designing Switchable Enzymes. *Curr. Opin. Struct. Biol.* **2009**, *19*, 442–448.
8. Koide, S. Generation Of New Protein Functions by Nonhomologous Combinations and Rearrangements of Domains and Modules. *Curr. Opin. Biotech.* **2009**, *20*, 398–404.
9. Giepmans, B. N.; Adams, S. R.; Ellisman, M. H.; Tsien, R. Y. The Fluorescent Toolbox for Assessing Protein Location and Function. *Science* **2006**, *312*, 217–224.
10. Isaacs, F. J.; Dwyer, D. J.; Collins, J. J. RNA Synthetic Biology. *Nat. Biotechnol.* **2006**, *24*, 545–554.
11. Sallee, N. A.; Yeh, B. J.; Lim, W. A. Engineering Modular Protein Interaction Switches by Sequence Overlap. *J. Am. Chem. Soc.* **2007**, *129*, 4606–4611.
12. Ma, B.; Kumar, S.; Tsai, C.; Nussinov, R. Folding Funnels and Binding Mechanisms. *Protein Eng.* **1999**, *12*), 713–720.
13. Tsai, C. J.; Ma, B.; Nussinov, R. Folding and Binding Cascades: Shifts in Energy Landscapes. *Proc. Natl. Acad. Sci. U.S.A.* **1999**, *96*, 9970–9972.
14. Kumar, S.; Ma, B.; Tsai, C.; Sinha, N.; Nussinov, R. Folding and Binding Cascades: Dynamic Landscapes and Population Shifts. *Protein Sc.* **2000**, *9*, 10–19.
15. Ma, B.; Shatsky, M.; Wolfson, H. J.; Nussinov, R. Multiple Diverse Ligands Binding at a Single Protein Site: a Matter of Pre-Existing Populations. *Protein Sc.* **2002**, *11*, 184–197.
16. Plaxco, K. W.; Soh, H. T. Switch Based Biosensors: a New Approach Towards Real-Time, *in Vivo* Molecular Detection. *Trends Biotechnol.* **2011**, *29*, 1–5.
17. Herschlag, D. The Role of Induced Fit and Conformational Changes of Enzymes in Specificity and Catalysis. *Bioorg. Chem.* **1988**, *16*, 62–96.
18. Vinkenborg, J. L.; Nicolson, T. J.; Bellomo, E. A.; Koay, M. S.; Rutter, G. A.; Merkx, M. Genetically Encoded FRET Sensors to Monitor Intracellular Zn^{2+} Homeostasis. *Nat. Methods.* **2009**, *6*, 737–740.
19. Johnson, K. A. Role of Induced Fit in Enzyme Specificity: A Molecular Forward/Reverse Switch. *J. Biol. Chem.* **2008**, *283*, 26297–26301.

20. Huang, J.; Koide, A.; Makabe, K.; Koide, S. Design of Protein Function Leaps by Directed Domain Interface Evolution. *Proc. Natl. Acad. Sci. U.S.A.* **2008**, *105*, 6578–6583.
21. Huang, J.; Makabe, K.; Biancalana, M.; Koide, A.; Koide, S. Structural Basis for Exquisite Specificity of Affinity Clamps, Synthetic Binding Proteins Generated Through Directed Domain-Interface Evolution. *J. Mol. Biol.* **2009**, *392*, 1221–1231.
22. Vallée-Bélisle, A.; Ricci, F.; Plaxco, K. W. Thermodynamic Basis for the Optimization of Binding-Induced Biomolecular Switches and Structure-Switching Biosensors. *Proc. Natl. Acad. Sci. U.S.A.* **2009**, *106*, 13802–13807.
23. Ricci, F.; Vallée-Bélisle, A.; Plaxco, K. W. High-Precision, *in Vitro* Validation of the Sequestration Mechanism for Generating Ultrasensitive Dose-Response Curves in Regulatory Networks. *PLoS Comp. Biol.* **2011**, *7*, e1002171.
24. Ricci, F.; Vallée-Bélisle, A.; Porchetta, A.; Plaxco, K. W. Rational Design of Allosteric Inhibitors and Activators Using the Population-Shift Model: *in Vitro* Validation and Application to an Artificial Biosensor. *J. Am. Chem. Soc.* **2012**, *134*, 15177–15180.
25. Vallée-Bélisle, A.; Ricci, F.; Plaxco, K. W. Engineering Biosensors With Extended, Narrowed, or Arbitrarily Edited Dynamic Range. *J. Am. Chem. Soc.* **2012**, *134*, 2876–2879.
26. Porchetta, A.; Vallée-Bélisle, A.; Plaxco, K. W.; Ricci, F. Using Distal-Site Mutations and Allosteric Inhibition to Tune, Extend, and Narrow the Useful Dynamic Range of Aptamer-Based Sensors. *J. Am. Chem. Soc.* **2012**, *134*, 20601–20604.
27. Kandimalla, E. R.; Agrawal, S. Single-Strand-Targeted Triplex Formation: Stability, Specificity and Rnase H Activation Properties. *Gene* **1994**, *149*, 115–121.
28. Kandimalla, E. R.; Manning, A.; Agrawal, S. Single Strand Targeted Triplex Formation: Physicochemical and Biochemical Properties of Foldback Triplexes. *J. Biomol. Str. Dyn.* **1996**, *14*, 79–90.
29. Kool, E. T. Preorganization of DNA: Design Principles for Improving Nucleic Acid Recognition by Synthetic Oligonucleotides. *Chem. Rev.* **1997**, *97*, 1473–1487.
30. Xodo, L. E.; Manzini, G.; Quadrifoglio, F. Spectroscopic and Calorimetric Investigation on the DNA Triplex Formed by D(CTCTTCTTTCTTTTCTTTCTTCTC) and D(GAGAAGAAAGA) at Acidic pH. *Nucleic Acids Res.* **1990**, *18*, 3557–3564.
31. Frank-Kamenetskii, M. D.; Mirkin, S. M. Triplex DNA Structures. *Annu. Rev. Biochem.* **1995**, *64*, 65–95.
32. Hoogsteen, K. The Structure of Crystals Containing a Hydrogen Bonded Complex of 1-Methylthymine and 9-Methyladenine. *Acta Crystallogr.* **1959**, *12*, 822–823.
33. Hoogsteen, K. The Crystal and Molecular Structure of a Hydrogen-Bonded Complex Between 1-Methylthymine and 9-Methyladenine. *Acta Crystallogr.* **1963**, *16*, 907–916.
34. Giovannangeli, C.; Thuong, N. T.; Helene, C. Oligonucleotide Clamps Arrest DNA Synthesis on a Single-Stranded DNA Target. *Proc. Natl. Acad. Sci. U.S.A.* **1993**, *90*, 10013–10017.
35. Trkulja, I.; Biner, S. M.; Langenegger, S. M.; Häner, R. A Molecular Probe for the Detection of Homopurine Sequences. *ChemBioChem* **2007**, *8*, 25–27.
36. Fatthalla, M. I.; Pedersen, E. B. Improved DNA Clamps by Stacking to Adjacent Nucleobases. *Helv. Chim. Acta* **2012**, *95*, 1538–1547.
37. Owczarzy, R.; Tataurov, A. V.; Wu, Y.; Manthey, J. A.; McQuisten, K. A.; Almabrazi, H. G.; Pedersen, F. K.; Lin, Y.; Garretson, J.; McEntaggart, N. O.; et al. IDT SciTools: A Suite for Analysis and Design of 572 Nucleic Acid Oligomers. *Nucleic Acids Res.* **2008**, *368*, 163–169.
38. Santalucia, J., Jr. A Unified View of Polymer, Dumbbell, and Oligonucleotide DNA Nearest-Neighbor Thermodynamics. *Proc. Natl. Acad. Sci. U.S.A.* **1998**, *95*, 1460–1465.
39. Santalucia, J., Jr.; Hicks, D. The Thermodynamics of DNA Structural Motifs. *Annu. Rev. Byophys. Biomol. Struct.* **2004**, *33*, 415–440.
40. Roberts, R.; Crothers, D. Prediction of The Stability of DNA Triplexes. *Proc. Natl. Acad. Sci. U.S.A.* **1996**, *93*, 4320–4325.
41. Volker, J.; Klump, H. H. Electrostatic Effect in DNA Triple Helices. *Biochemistry* **1994**, *33*, 13502–13508.
42. Best, G. C.; Dervan, P. B. Energetics of Formation of Sixteen Triple Helical Complexes Which Vary at a Single Position Within a Pyrimidine Motif. *J. Am. Chem. Soc.* **1195**, *117*, 1187–1193.
43. Marras, S. A. E.; Tyagi, S.; Kramer, F. R. Real-Time Assays With Molecular Beacons and Other Fluorescent Nucleic Acid Hybridization Probes. *Clin. Chim. Acta* **2006**, *363*, 48–60.
44. Ricci, F.; Plaxco, K. W. E-DNA Sensors for Convenient, Label-Free Electrochemical Detection of Hybridization. *Microchim. Acta* **2008**, *163*, 149–155.
45. Tyagi, S.; Bratu, D. P.; Kramer, F. R. Multicolor molecular beacons for allele discrimination. *Nat. Biotechnol.* **1998**, *16*, 49–53.
46. Zhang, D. Y.; Chen, S. X.; Yin, P. Optimizing the Specificity of Nucleic Acid Hybridization. *Nature Chem.* **2012**, *4*, 208–214.
47. Pace, C. N. Determination and Analysis of Urea and Guanidine Hydrochloride Denaturation Curves. *Meth. Enzymol.* **1986**, *131*, 266–280.
48. Shelton, V. M.; Sosnick, T. R.; Pan, T. Applicability of Urea in the Thermodynamic Analysis of Secondary and Tertiary RNA Folding. *Biochemistry* **1999**, *38*, 16831–16839.
49. Santoro, M. M.; Bolen, D. W. Unfolding Free Energy Changes Determined by the Linear Extrapolation Method. 1. Unfolding of Phenylmethanesulfonyl α-Chymotrypsin Using Different Denaturants. *Biochemistry* **1988**, *27*, 8063–8068.
50. Rossmann, M. G.; Moras, D.; Olsen, K. W. Chemical and Biological Evolution of Nucleotide Binding Protein. *Nature* **1974**, *250*, 194–199.
51. Blake, C. C. F. Do Genes-In-Pieces Imply Proteins-In-Pieces? *Nature* **1978**, *273*, 267–268 (52) Pawson, T.; Nash, P. Assembly of Cell Regulatory Systems Through Protein Interaction Domains. *Science* **2003**, *300*, 445–452.
52. Goñi, J. R.; de la Cruz, X.; Orozco, M. Triplex-Forming Oligonucleotide Target Sequences in the Human Genome. *Nucleic Acids Res.* **2004**, *32*, 354–360.
53. Duca, M.; Vekhoff, P.; Oussedik, K.; Halby, L.; Arimondo, P. B. The Triple Helix: 50 Years Later, the Outcome. *Nucleic Acids Res.* **2008**, *36*, 5123–5138.
54. Muller, J.; Wulffen, B.; Potzsch, B.; Mayer, G. Multidomain Targeting Generates a High-Affinity Thrombin-Inhibiting Bivalent Aptamer. *ChemBioChem.* **2007**, *8*, 2223–2226.
55. Yurke, B.; Turberfield, A. J.; Mills, A. P., Jr.; Simmel, F. C.; Neumann, J. L. A DNA-Fuelled Molecular Machine Made of DNA. *Nature* **2000**, *406*, 605–608.
56. Nimjee, S. M.; Rusconi, C. P.; Sullenger, B. A. Aptamers: an Emerging Class of Therapeutics. *Annu. Rev. Med.* **2005**, *56*, 555–583.
57. Seelig, G.; Soloveichik, D.; Zhang, D. Y.; Winfree, E. Enzyme-Free Nucleic Acid Logic Circuits. *Science* **2006**, *314*, 1585–1588.
58. Yin, P.; Choi, H. M. T.; Calvert, C. R.; Pierce, N. A. Programming Biomolecular Self-Assembly Pathways. *Nature* **2008**, *451*, 318–322.
59. Andersen, E. S.; Dong, M.; Nielsen, M. M.; Jahn, K.; Subramani, R.; Mamdouh, W.; Golas, M. M.; Sander, B.; Stark, H.; Oliveira, C. L. P.; et al. Self-Assembly of a Nanoscale DNA Box With a Controllable Lid. *Nature* **2009**, *459*, 73–76.
60. Keefe, A. D.; Pai, S.; Ellington, A. Aptamers as Therapeutics. *Nat. Rev. Drug Discovery* **2010**, *9*, 537–550.
61. Krishnan, Y.; Simmel, F. C. Nucleic Acid Based Molecular Devices. *Angew. Chem., Int. Ed.* **2011**, *50*, 3124–3156.